Cerebellum (2012) 11:1026–1036
DOI 10.1007/s12311-012-0379-1

ORIGINAL PAPER

Macrocerebellum: Significance and Pathogenic Considerations

Andrea Poretti · Volker Mall · Martin Smitka · Sebastian Grunt · Sarah Risen · Sandra P. Toelle · Jane E. Benson · Shoko Yoshida · Nikolai H. Jung · Sigrid Tinschert · Teresa M. Neuhann · Anita Rauch · Maja Steinlin · Avner Meoded · Thierry A. G. M. Huisman · Eugen Boltshauser

Published online: 14 April 2012

Abstract Macrocerebellum is a rare finding characterized by an abnormally large cerebellum. Only few patients with a syndromal or isolated macrocerebellum have been reported so far. This article aims to categorize the magnetic resonance imaging (MRI) findings, quantitate the macrocerebellum by volumetric analysis, characterize the neurological and dysmorphic features and cognitive outcome, and report the results of genetic analyses in children with macrocerebellum. All MR images were qualitatively evaluated for infratentorial and supratentorial abnormalities. Volumetric analysis was performed. Data about neurological and dysmorphic features, outcome, and genetic analysis were collected from clinical histories and follow-up examinations. Five patients were included. Volumetric analysis in three patients confirmed large cerebellar size compared to age-matched controls. MR evaluation showed that thickening of the cortical gray matter of the cerebellar hemispheres is responsible for the macrocerebellum. Additional infratentorial and supratentorial abnormalities were present in all patients. Muscular hypotonia, as well as impaired motor and cognitive development, was found in all patients, with ocular movement disorders in three of five patients. The five patients differed significantly in terms of dysmorphic features and involvement of extracerebral organs. Submicroscopic chromosomal aberrations were found in two

A. Poretti · S. P. Toelle · E. Boltshauser (✉)
Department of Pediatric Neurology,
University Children's Hospital of Zurich,
Steinwiesstrasse 75,
8032, Zurich, Switzerland
e-mail: Eugen.Boltshauser@kispi.uzh.ch

A. Poretti · J. E. Benson · A. Meoded · T. A. G. M. Huisman
Division of Pediatric Radiology, Russell H. Morgan Department of Radiology and Radiological Science,
The Johns Hopkins University School of Medicine,
Baltimore, MD, USA

V. Mall · N. H. Jung
Division of Neuropediatrics and Muscular Disorders,
Department of Pediatrics and Adolescent Medicine,
University Hospital Freiburg,
Freiburg, Germany

V. Mall · M. Smitka
Department of Pediatric Neurology, Pediatrics,
University Children's Hospital Carl Gustav Carus,
Dresden University of Technology,
Dresden, Germany

S. Grunt · M. Steinlin
Department of Pediatric Neurology,
University Children's Hospital of Bern,
Bern, Switzerland

S. Risen
Kennedy Krieger Institute,
Baltimore, MD, USA

S. Yoshida
Laboratory of Brain Anatomical MRI,
Russell H. Morgan Department of Radiology and Radiological Science, The Johns Hopkins School of Medicine,
Baltimore, MD, USA

S. Tinschert · T. M. Neuhann
Institute of Clinical Genetics,
Medical Faculty Carl Gustav Carus,
Dresden University of Technology,
Dresden, Germany

A. Rauch
Institute of Medical Genetics, University of Zurich,
Zurich, Switzerland

patients. Macrocerebellum is caused by thickening of the cortical gray matter of the cerebellar hemispheres, suggesting that cerebellar granule cells may be involved in its development. Patients with macrocerebellum show highly heterogeneous neuroimaging, clinical, and genetic findings, suggesting that macrocerebellum is not a nosological entity, but instead represents the structural manifestation of a deeper, more basic biological disturbance common to heterogeneous disorders.

Keywords Cerebellum · Macrocerebellum · Neuroimaging · Cognitive functions

Introduction

Macrocerebellum is a very rare finding and is characterized by an abnormally large cerebellum with preservation of its overall shape [1]. Its pathogenesis is unknown. Macrocerebellum may be part of a well-defined syndromal condition as Sotos syndrome [2], Costello syndrome [3], Williams syndrome [4], macrocephaly-capillary malformation syndrome [5, 6], Alexander disease [7, 8], fucosidosis [9], or Lhermitte–Duclos syndrome (Table 1) [10–12]. Additionally, patients with isolated (nonsyndromal) macrocerebellum have also been reported [13, 14].

This article aims to (1) characterize the neurological and dysmorphic features as well as the neurodevelopmental outcome, (2) evaluate the spectrum of neuroimaging findings, (3) quantitatively verify the qualitative evaluation of an increased cerebellar volume, and (4) present the results of genetic investigations in our cohort of patients with a macrocerebellum.

Patients and Methods

Patient Cohort

The patients included in this study were found by the senior author (EB) from three sources: (1) his personal database of patients with cerebellar abnormalities, (2) neuroimaging data of referred patients subsequently diagnosed with macrocerebellum, and (3) personal contacts with other clinical professionals who contributed cases. The inclusion criterion for this retrospective study was a qualitatively large cerebellum on MR images in midsagittal (large cerebellar vermis filling the posterior fossa with absence or decrease of the physiological retrovermian amount of cerebrospinal fluid (CSF)) or axial (large cerebellum filling the posterior fossa with absence or decrease of the physiological pericerebellar/retrocerebellar amount of CSF) planes.

Clinical Analysis

Review of the clinical histories and clinical–neurological follow-up examinations provided detailed information about neurological and dysmorphic features as well as neurodevelopmental outcome. These details are listed in Table 2.

Qualitative Neuroimaging Analysis

In a retrospective fashion, two pediatric neurologists with experience in neuroimaging of the pediatric cerebellum (AP and EB) qualitatively analyzed all available imaging data sets. The parameters chosen for evaluation are listed in Table 3.

Table 1 Differential diagnosis of macrocerebellum

Disease	OMIM	Additional neuroimaging findings	References
Sotos syndrome	#117550	Ventricular abnormalities, increased extracerebral fluid spaces, midline abnormalities, and migration anomalies	[2]
Costello syndrome	#218040	Macrocerebellum progressively causing cerebellar tonsillar herniation and hydrocephalus, Chiari 1, syrinx formation	[3]
Williams syndrome	#194050	"Small cerebrum"	[4]
Macrocephaly-capillary malformation	%602501	Hydrocephalus, asymmetric lateral ventricle, white matter defects, hemimegalencephaly, Chiari 1, polymicrogyria, cortical dysplasia	[5, 6]
Alexander disease	#203450	Symmetrical cerebral white matter abnormalities with a frontal preponderance, periventricular rim of decreased signal intensity on T2-weighted images, abnormalities of the basal ganglia, thalami, and brainstem, contrast enhancement involving several brain structures	[7, 8]
Fucosidosis	#230000	Hypomyelination and T1-weighted hyperintensity of putamina and globi pallidi	[9]
Lhermitte–Duclos syndrome	#158350	Non-enhancing gyriform pattern, hypointensity on T1-weighted images, striated pattern with isointense bands in the area of hyperintensity on T2-weighted images	[10–12]

Modified with permission from Poretti and Boltshauser [1]

Table 2 Clinical characteristics in five patients with macrocerebellum

	Patient 1	Patient 2	Patient 3	Patient 4	Patient 5
Gender	Male	Male	Female	Male	Female
Origin	Swiss	Swiss	German	German	US
Parental consanguinity	No	No	No	No	No
Siblings	No	No	2	2 half siblings	Healthy identical twin
Prenatal anomalies	No	No	No	Growth retardation	Ventriculomegaly
Gestational age at birth (weeks)	39 4/7	35 5/7	38	39 1/7	33 2/7
Age at first symptoms (months)	2	Neonate	Neonate	Neonate	Neonate
First symptoms	Delayed visual fixation	Small for date	Macrocephaly	Respiratory distress	Hydrocephalus
HC at presentation (centile)	25th	10th–25th	>>97th	25th	>>97th
Age at last follow-up (months)	36	18	30	37	12
HC at follow-up (centile)	<<3 rd	25th–50th	>97th	<3 rd	>97th
Muscle tone	Decreased	Axial decreased +++, limbs increased ++	Decreased +++	Decreased	Axial decreased +
Ataxia	Truncal and limb	n.a.	Truncal	n.a.	n.a.
Ocular movement disorders	Nystagmus	Downbeat nystagmus, horizontal > vertical gaze palsy, strabismus	No	Nystagmus	No
Epilepsy	Complex–partial seizures	No	No	Complex–partial seizures	Complex–partial seizures
Cognitive development	Impairment +++	Dev. delay +	Dev. delay +	Impairment +++	Dev. delay +
Speech/language	No speech	Delay +	Delay +	No speech	Normal
Other neurological findings	No	No	No	No fixation, bilat. optic atrophy	Occipital encephalocele
Dysmorphic signs	Small feet, short nose, thin upper lip	Low-set ears, retrognathia, prominent forehead, micropenis	Flat nasal bridge	Prominent forehead, short nose, deep-set eyes, thin upper lip	No
Other clinical findings	No	Panhypopituitarism, failure to thrive	Hyperopia +++ (+7.0 dioptres)	No	Scalp cutis aplasia congenita, small VSD
VP shunt (if yes → age)	No	No	8 months	No	4 days

Bilat. bilateral, *Dev.* developmental, *HC* head circumference, *n.a.* not applicable, *VP* ventriculoperitoneal, *VSD* ventricular septal defect, + mild, ++ moderate, +++ marked

Table 3 Neuroimaging findings in five patients with macrocerebellum

	Patient 1	Patient 2	Patient 3	Patient 4	Patient 5
Age at last MRI (months)	7	19	26	10	12
Size of the cerebellar GM	↑	↑	↑	↑	↑
Size of the cerebellar WM	↓	=	=	=	=
Vermis size	=	IVH	=	=	=
Cerebellar dysplasia	Yes	No	No	No	No
Herniation of the cerebellar tonsils	No	No	Yes	No	No
Wrapping of the cerebellar hemispheres around the brainstem	No	Yes	Yes	No	Yes
Cerebellar WM signal abnormalities	No	No	Yes	No	No
Size/shape of the fourth ventricle	=	↓, upwards displaced	Mildly ↓	Mildly ↓	Mildly upwards displaced
Brainstem structural abnormalities (morphology)	Mes. elongated/thickened, short pons	Premesencephalic heterotopia, pons shortened	Mes. thickened	No	Tectal "beaking"
Posterior fossa subarachnoid spaces	Wide prepontine cistern	Cerebellopontine angle AC left	Narrow prepontine cistern	Paracerebellar AC right	Narrow prepontine cistern
Ventriculomegaly/hydrocephalus	++	+, VP shunt	+++	+++	+++, VP shunt
Corpus callosum dysgenesis	No	No	No	No	Yes
Supratentorial migrational disorders	Frontal gyral pattern ↓, PH	No	No	No	Subependymal heterotopia
Supratentorial WM abnormalities	No	Delayed myelination +	Diffuse T2 hyperintensity	Global volume loss +++	Global volume loss ++
Additional findings	No	Horizontal SCP, flat sella, ectopic neurohypophysis, absent adenohypophysis	No	Thin optic pathway	Upwards cerebellar herniation, no septum pellucidum, partially fused thalami, occipital encephalocele

AC arachnoid cyst, *GM* gray matter, *IVH* inferior vermis hypoplasia, *Mes.* mesencephalon, *PH* periventricular heterotopia, *SCP* superior cerebellar peduncles, *VP shunt* ventriculoperitoneal shunt, *WM* white matter, ↑ increased, ↓ reduced, = normal, + mild, ++ moderate, +++ marked

Volumetric Analysis

Volumetric analysis was performed using axial and sagittal 3D T1-weighted images. These were available for three patients. Five age- and gender-matched Caucasian controls were selected for every patient from the pediatric MR database at Johns Hopkins Hospital using the following criteria: (1) normal brain anatomy, (2) absence of neurological disorders, and (3) availability of 3D T1-weighted images. We decided not to use control data about the cerebellar volume from the literature [9, 15] because of different post-processing methods. For the off-line post-processing, we used DtiStudio, DiffeoMap, and RoiEditor software (H. Jiang and S. Mori, Johns Hopkins University, available at http://www.MriStudio.org) as well as FSL software (The University of Oxford, available at http://www.fmrib.ox.ac.uk). The post-processing was performed by AP and SY.

First, atlas-based normalization was performed for the images of control 3 to create a template with structural parcellation for this study. This control was chosen because the age corresponded most closely to the JHU-DTI-MNI "Eve" template (a single-subject template in the ICBM-DTI-81 space that is extensively parcellated and labeled into 130 structures). After skull-stripping using RoiEditor and FSL, the images were first normalized to the "Eve" template with a nine-parameter affine linear transformation. Subsequently, a nonlinear transformation using single-contrast (T1-weighted images) large deformation diffeomorphic metric mapping was applied [16]. Because both linear and nonlinear transformations are reciprocal procedures, the inversely transformed brain parcellation map was superimposable onto the original 3D T1-weighted images from control 3, leading to the parcellation of the brain into 130 anatomical structures.

Next, for the 3D T1-weighted images of the other controls and patients, we performed the same atlas-based transformation using the image of control 3 as the template, followed by minimum manual adjustment. As a result, the quantitative volume values (number of voxels) for 130 parcellated brain structures were obtained for each patient and control.

Among 130 parcellated brain structures, the total number of voxels of the cerebellar regions (region no. 28, "cerebellum left"; region no. 50, "middle cerebellar peduncles left"; region no. 93, "cerebellum right"; region no. 115, "middle cerebellar peduncles right") was used to calculate the cerebellar volume. The right half of the cerebellar vermis is included within the region "cerebellum right" and the left one within the region "cerebellum left." The middle cerebellar peduncles were included into the volume calculation because they are a significant part of the cerebellar volume. Because every voxel measures $1 \times 1 \times 1$ mm, the cerebellar volume was measured in cubic millimeters.

Genetic Studies

Genetic analyses included (1) cytogenetic karyotyping of metaphases from peripheral blood lymphocytes by GTG banding analysis, (2) molecular karyotyping by single nucleotide polymorphism (SNP) array with an Affymetrix 100 K Nsp Gene Chip Array (patient 1) and Illumina Human Quad 610 BeadChip containing 610,000 SNPs (patient 5) and by high-resolution oligonucleotide array comparative genomic hybridization (CGH) analysis with a Roche Nimblegen Human CGH Microarray Kit 135 (patient 2), BlueGnome Human CGH Microarray Cytochip v1.0 Kit 180 (patient 3), and Agilent's Human CGH Microarray Kit 244A (patient 4), and (3) mutation analysis for selected genes (patients 1 and 3).

Results

Patient Characteristics

Five Caucasian patients were included in this study. At the last follow-up, the median age was 33 months (mean, 27 months; range, 12 to 37 months). The patient characteristics are included in Table 2. Clinical and genetic findings of patient 4 were included in a previous report [17].

Clinical Findings

The clinical, neurological, and dysmorphic characteristics of the five patients with macrocerebellum are summarized in Table 2. Ataxia could not be evaluated for patients 2, 3, and 5 because of the developmental age.

Detailed data on motor and/or cognitive development were abnormal in all patients. At the age of 36 months, patient 1 was able to roll over serially and grasp at toys (and throw them away immediately), but was not able to feed himself. He understood a few simple tasks and had no speech, though showed his agreement/refusal by head movements. The estimated developmental age was 9 months (corresponding to a developmental quotient (DQ) of 25). The DQ of patient 2, measured at the age of 18 months with the Griffiths Mental Developmental Scale, was 69 (corresponding to a developmental age of 12.4 months). His motor abilities corresponded to a developmental age of 7 months (rolling over serially, but not able to sit). His hearing and speech ability corresponded to 12 months, his performance ability to 12.5 months, eye–hand coordination ability to 13.5 months, and personal–social ability to 14 months. At the age of 18 months, patient 3 appeared interested and active. She spoke only about 10 words, was able to grasp at toys, stand up, and walk around, though only with support. The estimated developmental age was

14 months (corresponding to a DQ of 77). At the age of 20 months, patient 4 was not able to stand or fix his gaze on an object and follow it, but could produce a few incomprehensible sounds. During further follow-up, patient 4 did not achieve new significant developmental milestones. The estimated developmental age was 3 months (corresponding to a DQ of 8). Finally, the DQ of patient 5 was measured at the corrected age of 5 months with the Clinical Adaptive Test and the Clinical Linguistic and Auditory Milestone Scale: the DQ for the cognitive portion was 92 (corresponding to a developmental age of 4.6 months), while the DQ for language was 86 (corresponding to a developmental age of 4.3 months). At the corrected age of 12 months, she was able to sit briefly, but not able to get to sitting position without assistance, crawl forward, or stand momentarily without support. She used pincer grasp, was able to exchange objects, and said "mama" and "dada." The achieved developmental milestones suggest a mild developmental delay, but the child is still very young for a conclusive evaluation.

Qualitative Neuroimaging Findings

Results of the qualitative neuroimaging analysis of each patient's most recent magnetic resonance imaging (MRI) (median age, 14 months; mean, 15 months; range, 7 to 27 months) are summarized in Table 3 and shown in Figs. 1, 2, 3, 4, and 5. Patients 3 and 5 had hydrocephalus: in patient 5, Sylvian aqueduct occlusion (not secondary to compression by the macrocerebellum) was the most likely cause, whereas in patient 3, the etiology was postulated to be macrocerebellum (obstructing the CSF circulation at the level of the posterior fossa) and/or herniation of the cerebellar tonsils. Additionally, in patient 5, the corpus callosum was very thin in its posterior part and the most anterior part appeared underdeveloped.

For patients 2, 3, and 5 additional prior MR images at the age of 12 months; 8, 11, and 17 months; and 2 days, respectively, were available. In all patients, the cerebellar findings were consistent on the follow-up images. Additionally, in patient 2, myelination of the white matter slightly improved. In patient 3, ventriculomegaly and diffuse, supratentorial T2 hyperintense signal abnormalities of the white matter were stable. In patient 5, the size of the lateral ventricles decreased significantly after placement of a ventriculoperitoneal shunt.

Volumetric Findings

Volumetric analysis was performed in three patients (patients 1–3; mean age, 9.6 months; median age, 11 months) and 15 age- and gender-matched controls (mean age, 9.6 months; median age, 11 months). In patient 4, volumetric analysis could not be performed because 3D T1-weighted images were not available; in patient 5, susceptibility artifacts related to the ventriculoperitoneal shunt degraded the images. The results are shown in Table 4. The mean cerebellar volume for controls 1a–e is 68,670 (SD, 2,278), for controls 2a–e is 102,777 (SD, 1,578), and for controls 3a–e is 97,271 (SD, 1,917). The ratio between the sum of the cerebellar volumes of the patients and the sum of the mean cerebellar volumes of the three control groups is 1.49. No statistical analysis was performed because of the small number of patients and controls.

Genetic Findings

Cytogenetic karyotyping at 400–550 band resolutions (ISCN 2009) was normal in all patients. Molecular karyotyping was normal in patients 1, 2, and 3, but revealed compound heterozygosity for a recurrent 1.5-Mb deletion within chromosome 15q13.3 and a 3.4-Mb deletion in 15q13.1–q13.3, resulting in

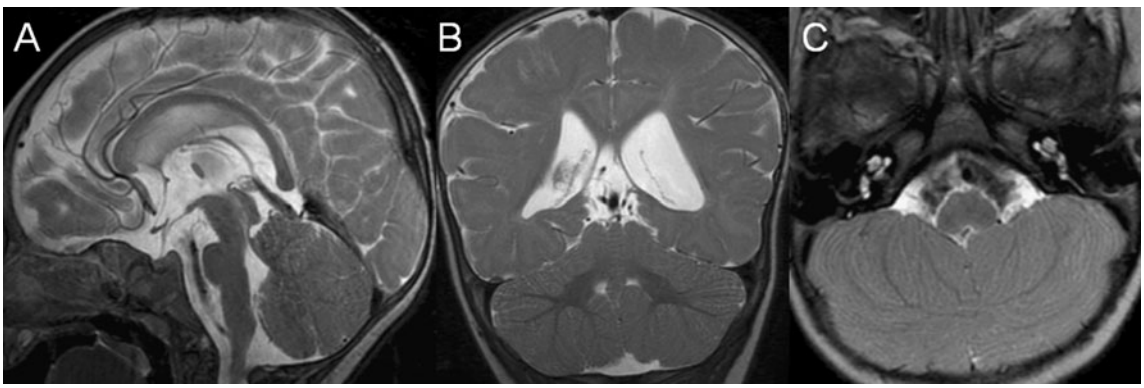

Fig. 1 Midsagittal (**a**), coronal (**b**), and axial (**c**) T2-weighted MR images of patient 1 at the age of 7 months show macrocerebellum with marked thickening of the cerebellar gray matter, but a mild volume decrease of the cerebellar white matter. Additional abnormalities illustrated: mild cerebellar dysplasia involving the posterior part of the hemispheres (**c**), an elongated and thickened mesencephalon (**a**), a short pons (**a**), a wide prepontine cistern (**a**), and a moderate ventriculomegaly (**b**). Reprinted with permission from Poretti and Boltshauser [1]

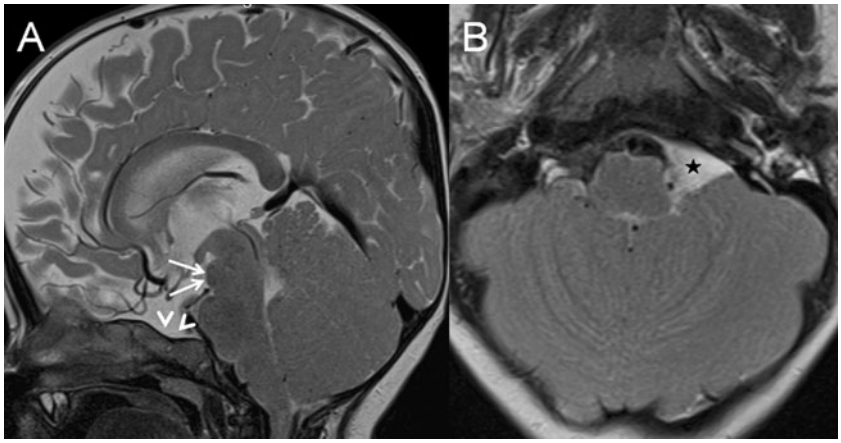

Fig. 2 Midsagittal (**a**) and axial (**b**) T2-weighted MR images of patient 2 at the age of 11 months show macrocerebellum with a marked thickening of the cerebellar gray matter (**b**), but a normal amount of cerebellar white matter (not shown). Additionally, size reduction and upward displacement of the fourth ventricle (**a**), premesencephalic heterotopia (*white arrows* in **a**), an arachnoid cyst in the left cerebellopontine angle (*black asterisk* in **b**), and a flat sella (*white arrowheads* in **a**) are noted

homozygous loss of the *CHRNA7* gene in patient 4 [6], and a 1.2-Mb heterozygous duplication on chromosome 1q42.3–q43 extending from 234,006,469 to 235,244,194 on build HG18 or NCBI36 in patient 5. Mutations could not be found within the *MECP2*, *CDKL5*, *ARX*, *NTNG1*, and *PHF6* genes in patient 1 or the *NSD1* gene in patient 3. Patient 5 has a healthy identical twin, but molecular cytogenetic analysis is not available for the twin and parents.

Discussion

A "small", hypoplastic cerebellum is not an unusual finding in pediatric neuroimaging. Reports suggest etiologies including prenatal infections, prenatal teratogen exposure, chromosomal aberrations, metabolic disorders and genetic (isolated or complex) brain malformations including migration disorders, some forms of congenital muscular dystrophies, and pontocerebellar hypoplasia [18]. A "large" cerebellum, on the other hand, is a very rare finding and has been inconsistently reported in few syndromes (Table 1) [3–12]. In all these syndromes, macrocerebellum is associated with additional characteristic clinical and/or neuroimaging findings which usually lead to the correct diagnosis. None of the patients included in our cohort, however, matched the characteristic clinical and neuroimaging findings of the syndromal conditions reported above.

Beyond these syndromes, macrocerebellum has been reported in only one additional patient cohort and in a single case (Table 5). Bodensteiner et al. reported four patients (age range, 9 months to 2 years) presenting with global developmental delay, muscular hypotonia, and ocular motor apraxia [13]. Additionally, deficient or delayed myelination of cerebral white matter was found in all patients. Picchiecchio et al. reported about a 19-month-old child with agenesis of the corpus callosum, who showed progressive enlargement of the cerebellum on sequential imaging studies [14]. The clinical examination revealed microcephaly, strabismus, global muscular hypertonia, developmental delay (DQ of 50), and dysmorphic features.

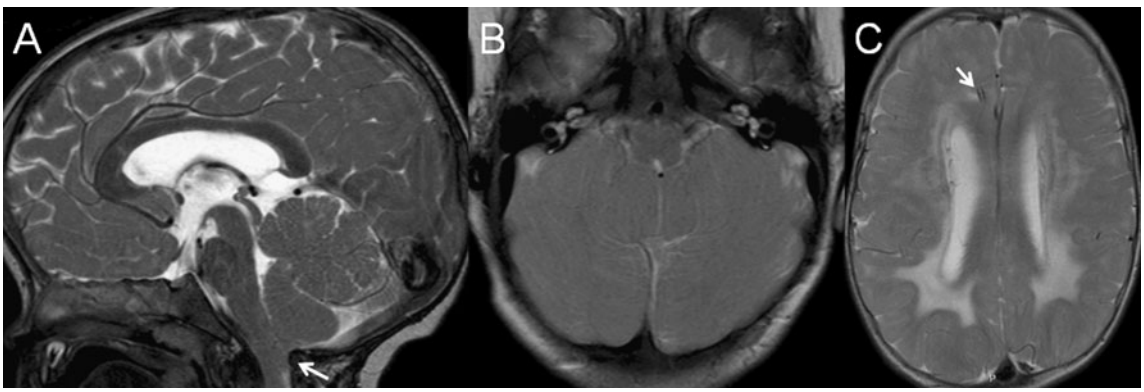

Fig. 3 Midsagittal (**a**) and axial (**b**) T2-weighted MR images of patient 3 at the age of 8 months show macrocerebellum with a marked thickening of the cerebellar gray matter, a size reduction of the fourth ventricle, a downward herniation of the cerebellar tonsils (*white arrow* in **a**), a narrow prepontine cistern, and a thickened mesencephalon. A supratentorial axial T2-weighted image (**c**) shows diffuse T2 hyperintense signal abnormality of the periventricular white matter is noted. Additionally, notice the patent Sylvian aqueduct (**a**) and the ventricular catheter of the ventriculoperitoneal shunt (*white arrow* in **c**)

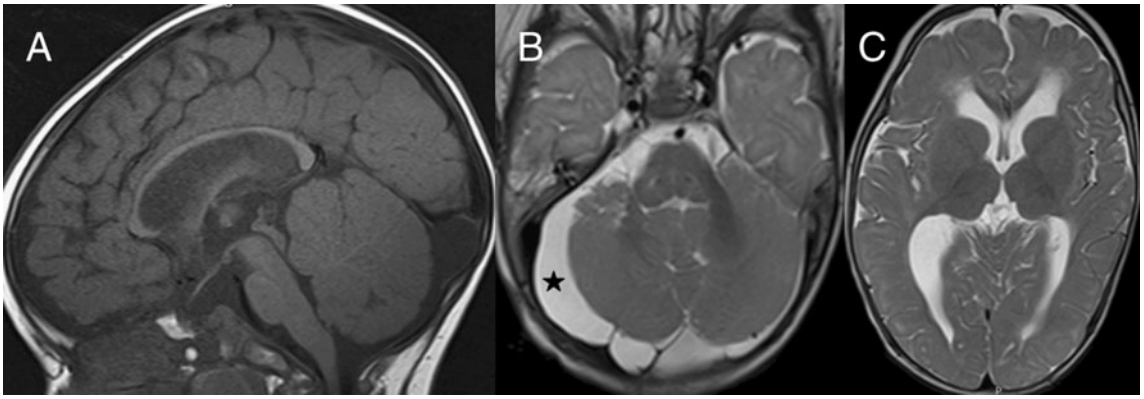

Fig. 4 Midsagittal (**a**) and axial (**b**) T2-weighted MR images of patient 4 at the age of 10 months show a macrocerebellum with a marked increase of the cerebellar gray matter. Additionally, a size reduction of the fourth ventricle (**a**), a right paracerebellar arachnoid cyst (*black asterisk* in **b**), and a thin corpus callosum (**a**) are noted. On the supratentorial axial T2-weighted image (**c**), a marked and diffuse volume loss of the white matter is noted

The majority of our patients presented during the neonatal period because of different problems including macrocephaly, hydrocephalus, or respiratory distress. The patient reported by Picchiecchio et al. presented also at birth because of craniofacial dysmorphic features [14].The patients of Bodensteiner et al., on the other hand, were slightly older (9 months to 2 years) and with more homogenous symptoms and findings [13]. At the last follow-up, all of our patients had muscular hypotonia, whereas ocular movement disorders, ataxia, and epilepsy were less common findings. Picchiecchio et al. reported global muscular hypertonia in their patient, but no epileptic seizures or ocular movement disorders [14], whereas all patients of Bodensteiner et al. had muscular hypotonia, decreased coordination, and ocular movement disorders, but no epileptic seizures [13]. Muscular hypotonia and ocular movement disorders are present in the majority of the patients and could represent the neurological presentation of children with a macrocerebellum. These neurological signs are, however, highly nonspecific and may be found in many other pediatric neurological disorders.

All our patients, as well as those reported by Bodensteiner et al. and Picchiecchio et al., have some degree of impairment in motor and cognitive development. It is well-known that small or structurally abnormal cerebellum results in motor and cognitive maldevelopment [19, 20]. Supratentorial abnormalities may also cause impairment of motor and cognitive development. Implicating macrocerebellum alone as a cause of delay in the three study cohorts is difficult because of the frequency of supratentorial abnormalities in these patients. However, the role of macrocerebellum cannot be discounted and could well have a negative effect comparable that of the other known structural cerebellar and supratentorial abnormalities. Of course, the

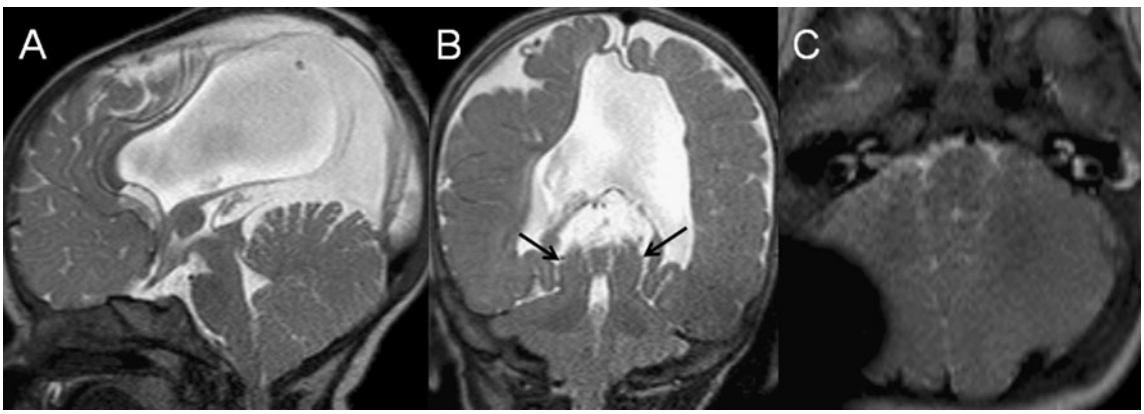

Fig. 5 Midsagittal (**a**), coronal (**b**), and axial (**c**) T2-weighted MR images of patient 5 at the age of 12 months show a macrocerebellum with a marked increase of the cerebellar gray matter (**c**). Additional abnormalities: mild upward displacement of the fourth ventricle (**a**), an upward herniation of the vermis and paravermian cerebellar tissue through the tentorium (*black arrows* in **b**), wrapping of the cerebellar hemispheres around the brainstem (**c**), a "beak-like" appearance of the tectum (**a**), a narrow prepontine cistern (**a**), a thin and dysplastic corpus callosum (**a**), and absence of the septum pellucidum (**b**). The Sylvian aqueduct is occluded (**a**). Imaging of the right cerebellar hemisphere is markedly disturbed by susceptibility artifacts related to the ventriculoperitoneal shunt

Table 4 Results of cerebellar volumetric studies in three patients with macrocerebellum and age- and gender-matched controls

	Gender	Age at MRI (months)	Volume (mm^3)				
			Cerebellum left	Cerebellum right	MCP left	MCP right	Total
Patient 1	Male	7	44,631	45,067	2,746	3,016	95,460
Patient 2	Male	11	60,626	58,162	5,080	5,789	129,657
Patient 3	Female	11	82,245	84,596	5,416	5,123	177,380
Control 1a	Male	7	32,926	33,010	2,110	2,099	70,146
Control 1b	Male	7	30,371	32,153	2,174	2,194	66,891
Control 1c	Male	7	31,362	31,307	2,058	2,183	66,910
Control 1d	Male	7	31,524	31,822	2,098	1,998	67,443
Control 1e	Male	7	33,504	34,191	2,122	2,142	71,959
Control 2a	Male	11	47,961	46,688	4,298	4,362	103,309
Control 2b	Male	11	46,062	47,091	4,241	4,265	101,658
Control 2c	Male	11	48,768	47,899	4,337	4,286	105,291
Control 2d	Male	11	46,908	46,438	4,068	4,051	101,465
Control 2e	Male	11	47,288	46,575	4,181	4,116	102,160
Control 3a	Female	11	43,235	45,004	3,664	4,240	96,143
Control 3b	Female	11	44,310	46,306	3,579	4,025	98,221
Control 3c	Female	11	43,675	44,269	3,990	3,431	95,365
Control 3d	Female	11	45,813	43,759	3,493	3,416	96,480
Control 3e	Female	11	47,326	45,876	3,340	3,605	100,147

MCP middle cerebellar peduncles

follow-up time is short and the patients were very young at the time of assessment.

Four of our patients had a variety of dysmorphic signs and two had involvement of extracerebral organs. The patient of Picchiecchio et al. as well as those of Bodensteiner et al. showed craniofacial dysmorphic signs, but no involvement of extracerebral organs [13, 14]. Thus, a specific pattern of craniofacial dysmorphic features or other malformations predicting macrocerebellum does not appear to be present.

The pathogenesis of macrocerebellum is still unknown. The qualitative evaluation of our patients with macrocerebellum showed that the large cerebellar size is caused by enlargement of the cerebellar hemispheres rather than of the cerebellar vermis. In one patient, we even found hypoplasia of the inferior vermis. Matching our observation, Bodensteiner et al. did not find a statistically significant difference between patients and controls when comparing two-dimensional morphometric measurement of the vermis [13]. This suggests that the vermis might be less affected by the process leading to a macrocerebellum. Interestingly, the posterior fossa never shows compensatory enlargement. Rather, the cerebellar hemispheres expand into adjacent anatomical regions by wrapping around the brainstem and herniating upward or downward.

In our patients, qualitative evaluation of cerebellar architecture revealed that the large size of the cerebellar hemispheres is caused by thickening of the cerebellar gray matter, while the volume of the cerebellar white matter appears normal or even reduced. The other two publications did not report this observation, and review of their published images does not suggest that this is present [13, 14]. Figures 1, 2, 3, 4, and 5 conversely show a striking imbalance in the normal proportions of gray to white matter. Why this was not a feature of the other two study cohorts is unknown, but this might point to a biologic avenue of investigation.

Cerebellar granule cells are one of the two main cellular populations in the cortical cerebellar gray matter [21]. Inactivation of *Pten* in specific mouse neuronal populations results in progressive increase in size of the granule cells, giving cerebellar abnormalities closely resembling the histopathology of human Lhermitte–Duclos syndrome [22, 23]. Lhermitte–Duclos syndrome is characterized by hypertrophy of the cerebellar cortex [10–12]. Though this hypertrophy is focal, not the global thickening seen in the present study group, it is still an intriguing example of this histopathologic mechanism. Genes encoding direct regulators of the cell cycle are critical for proper proliferation of granule cells [24]. *Cyclin D2* is a positive regulator of the cell cycle. Its inactivation in mice causes reduction of the granule cell population because of decreased proliferation and increased apoptosis of granule progenitors and results in cerebellar hypoplasia [25]. On the other hand, inactivation of *p27Kip1*, a negative regulator of the cell cycle, results in an increased proliferation of granule cells and formation of a large cerebellum [26]. Additional

Table 5 Clinical and neuroimaging characteristics in five published patients with macrocerebellum

	Patient 1	Patient 2	Patient 3	Patient 4	Patient 5
Author	Bodensteiner [13]	Bodensteiner	Bodensteiner	Bodensteiner	Pichiecchio [14]
Gender	Male	Female	Male	Male	Male
Age (months)	30	24	11	9	19
HC (head circumference)	Normal	Decreased	Decreased	Normal	Decreased
Muscle tone	Decreased	Variable	Decreased	Decreased	Increased
Ataxia	No	No	No	No	n.a.
Ocular movement disorders	OMA	OMA	Unknown	OMA	Left eye squint
Epilepsy	No	No	No	No	No
Motor development delay	++	+++	+	++	DQ 50
Cognitive development delay	++	+++	++	+++	
Other neurological findings	No	Brisk reflexes	No	No	Ptosis, poor facial mimic, brisk reflexes
Dysmorphic signs	Yes	Yes	Yes	No	Yes
Vermis size	Increased	Normal	Increased	Increased	Unknown
Cerebellar dysplasia	No	No	No	No	No
Cerebellar white matter	Normal	Normal	Normal	Normal	Normal
Supratentorial white matter	Delayed myelination	Delayed myelination	Delayed myelination	Delayed myelination	Delayed myelination
Additional neuroimaging findings	No	No	No	No	Corpus callosum agenesis

DQ developmental quotient, *MRI* magnetic resonance imaging, *n.a.* not applicable, *OMA* ocular motor apraxia, + mild, ++ moderate, +++ marked

genes, as well as environmental substances, may also play a role in regulating cell number or influencing neurogenesis and gliogenesis in the embryonic and postnatal brain, but their involvement in the pathogenesis of macrocerebellum has not been demonstrated so far [18].

Molecular cytogenetic studies revealed submicroscopic chromosomal anomalies in two patients of our cohort. The compound heterozygous deletions on chromosome 15q13 in patient 4 included a homozygously deleted segment in 15q13.3 that encompasses the *CHRNA7* gene. Patients with homozygous deletions of the *CHRNA7* gene can present with refractory epileptic seizures, cognitive impairment, severe muscular hypotonia, autistic features, choreoathetotic movements, and congenital retinal dysfunction [17, 27–29]. Neuroimaging findings in five additional patients with homozygous deletions of the *CHRNA7* gene included multiple arachnoid cysts in three patients and bilateral frontal volume loss in two patients, while MRI was normal in one patient [17, 27–29]. Heterozygous 15q13.3 microdeletions have been identified as a predisposition to cognitive impairment, epilepsy, and psychiatric diseases [27]. The significance of the small heterozygous duplication on chromosome 1q42.3–q43 in patient 5 remains unclear because molecular cytogenetic studies are not available for the twin and parents. Macrocerebellum, however, has not been described in patients with 15q13.3 microdeletions as well as submicroscopic chromosomal anomalies on the long arm of chromosome 1. It is plausible that macrocerebellum may be due not only to different expressions of genetic aberrations, but also to disturbances at different stages of cerebellar development. In patient 5, macrocerebellum was present already at 2 days of age. In the patient reported by Pichiecchio et al., however, cerebellar size was normal during the neonatal period and macrocerebellum was detected first at the age of 19 months [14].

We are aware of some limitations in our study. Although this is the largest reported cohort, the number of patients with macrocerebellum is still small. Additionally, the follow-up time is short. Moreover, volumetric analysis was only performed in three patients. Finally, the DQ was only measured in two patients using standardized developmental tests.

Conclusions

Macrocerebellum is a qualitatively recognizable finding on neuroimaging and is quantitatively verifiable. Comparison of these 10 cases points out the heterogeneous clinical and imaging context in which it is seen. There is likely a biologic explanation—possibly involving granule cell growth—that in turn may link the disparate syndromes in which it is seen. More patients need to be studied; it is hoped that this paper will stimulate the search for these patients and facilitate recognition of macrocerebellum as a recordable diagnostic observation.

Acknowledgments We thank the patients and their families for their cooperation. We are grateful to Dr. G. Hahn, Department of Pediatric Radiology, Children's Hospital, Dresden, Germany for the neuroimaging data of a patient and Prof. Dr. A. Hamosh, Institute of Genetic Medicine, Johns Hopkins University School of Medicine, Baltimore, MD, USA for the genetic data of a patient. This work was supported by the Anna Müller Grocholski Foundation, Zurich, Switzerland (A.P.).

Conflict of Interest We declare that we have no conflicts of interest.

References

1. Poretti A, Boltshauser E. Macrocerebellum. In: Boltshauser E, Schmahmann JD, editors. Cerebellar disorders in children. London: Mac Keith Press; 2012. p. 192–3.
2. Schaefer GB, Bodensteiner JB, Buehler BA, Lin A, Cole TR. The neuroimaging findings in Sotos syndrome. Am J Med Genet. 1997;68:462–5.
3. Gripp KW, Hopkins E, Doyle D, Dobyns WB. High incidence of progressive postnatal cerebellar enlargement in Costello syndrome: brain overgrowth associated with HRAS mutations as the likely cause of structural brain and spinal cord abnormalities. Am J Med Genet A. 2010;152A:1161–8.
4. Jones W, Hesselink J, Courchesne E, Duncan T, Matsuda K, Bellugi U. Cerebellar abnormalities in infants and toddlers with Williams syndrome. Dev Med Child Neurol. 2002;44:688–94.
5. Conway RL, Pressman BD, Dobyns WB, et al. Neuroimaging findings in macrocephaly-capillary malformation: a longitudinal study of 17 patients. Am J Med Genet A. 2007;143A:2981–3008.
6. Conway RL, Danielpour M, Graham Jr JM. Surgical management of cerebellar tonsillar herniation in three patients with macrocephaly-cutis marmorata telangiectatica congenita. Report of three cases. J Neurosurg. 2007;106:296–301.
7. Torreman M, Smit LM, van der Valk P, Valk J, Scheltens P. A case of macrocephaly, hydrocephalus, megacerebellum, white matter abnormalities and Rosenthal fibers. Dev Med Child Neurol. 1993;35:732–6.
8. van der Knaap MS, Salomons GS, Li R, et al. Unusual variants of Alexander's disease. Ann Neurol. 2005;57:327–38.
9. Kau T, Karlo C, Gungor T, et al. Increased cerebellar volume in the early stage of fucosidosis: a case control study. Neuroradiology. 2011;53:509–16.
10. Milbouw G, Born JD, Martin D, et al. Clinical and radiological aspects of dysplastic gangliocytoma (Lhermitte–Duclos disease): a report of two cases with review of the literature. Neurosurgery. 1988;22:124–8.
11. Nowak DA, Trost HA. Lhermitte–Duclos disease (dysplastic cerebellar gangliocytoma): a malformation, hamartoma or neoplasm? Acta Neurol Scand. 2002;105:137–45.
12. Perez-Nunez A, Lagares A, Benitez J, et al. Lhermitte–Duclos disease and Cowden disease: clinical and genetic study in five patients with Lhermitte–Duclos disease and literature review. Acta Neurochir (Wien). 2004;146:679–90.
13. Bodensteiner JB, Schaefer GB, Keller GM, Thompson JN, Bowen MK. Macrocerebellum: neuroimaging and clinical features of a newly recognized condition. J Child Neurol. 1997;12:365–8.
14. Pichiecchio A, Di Perri C, Arnoldi S, et al. Cerebellum enlargement and corpus callosum agenesis: a longitudinal case report. J Child Neurol. 2011;26:756–60.
15. Wu KH, Chen CY, Shen EY. The cerebellar development in Chinese children—a study by voxel-based volume measurement of reconstructed 3D MRI scan. Pediatr Res. 2011;69:80–3.
16. Miller MI, Beg MF, Ceritoglu C, Stark C. Increasing the power of functional maps of the medial temporal lobe by using large deformation diffeomorphic metric mapping. Proc Natl Acad Sci U S A. 2005;102:9685–90.
17. Endris V, Hackmann K, Neuhann TM, et al. Homozygous loss of CHRNA7 on chromosome 15q13.3 causes severe encephalopathy with seizures and hypotonia. Am J Med Genet A. 2010;152A:2908–11.
18. Poretti A, Boltshauser E. Cerebellar hypoplasia. In: Boltshauser E, Schmahmann JD, editors. Cerebellar disorders in children. London: Mac Keith Press; 2012. p. 121–34.
19. Steinlin M. Cerebellar disorders in childhood: cognitive problems. Cerebellum. 2008;7:607–10.
20. Bolduc ME, Limperopoulos C. Neurodevelopmental outcomes in children with cerebellar malformations: a systematic review. Dev Med Child Neurol. 2009;51:256–67.
21. Ten Donkelaar HJ, Lammens M. Development of the human cerebellum and its disorders. Clin Perinatol. 2009;36:513–30.
22. Backman SA, Stambolic V, Suzuki A, et al. Deletion of Pten in mouse brain causes seizures, ataxia and defects in soma size resembling Lhermitte–Duclos disease. Nat Genet. 2001;29:396–403.
23. Kwon CH, Zhu X, Zhang J, et al. Pten regulates neuronal soma size: a mouse model of Lhermitte–Duclos disease. Nat Genet. 2001;29:404–11.
24. Chizhikov V, Millen KJ. Development and malformations of the cerebellum in mice. Mol Genet Metab. 2003;80:54–65.
25. Huard JM, Forster CC, Carter ML, Sicinski P, Ross ME. Cerebellar histogenesis is disturbed in mice lacking cyclin D2. Development. 1999;126:1927–35.
26. Miyazawa K, Himi T, Garcia V, Yamagishi H, Sato S, Ishizaki Y. A role for p27/Kip1 in the control of cerebellar granule cell precursor proliferation. J Neurosci. 2000;20:5756–63.
27. Masurel-Paulet A, Andrieux J, Callier P, et al. Delineation of 15q13.3 microdeletions. Clin Genet. 2010;78:149–61.
28. Liao J, Deward SJ, Madan-Khetarpal S, Surti U, Hu J. A small homozygous microdeletion of 15q13.3 including the CHRNA7 gene in a girl with a spectrum of severe neurodevelopmental features. Am J Med Genet A. 2011;155:2795–800.
29. Spielmann M, Reichelt G, Hertzberg C, et al. Homozygous deletion of chromosome 15q13.3 including CHRNA7 causes severe mental retardation, seizures, muscular hypotonia, and the loss of KLF13 and TRPM1 potentially cause macrocytosis and congenital retinal dysfunction in siblings. Eur J Med Genet. 2011;54:e441–5.